

IMPROVED METHOD FOR SIMULATING FRICTIONAL LOSSES IN LAMINAR TRANSIENT LIQUID PIPE FLOW

KAMIL URBANOWICZ, ZBIGNIEW ZARZYCKI
AND SYLWESTER KUDŹMA

*Faculty of Mechanical Engineering and Mechatronics,
Mechanical Department,*

*Szczecin West Pomeranian University of Technology,
Piastów 19, 70-310 Szczecin, Poland*

{Kamil.Urbanowicz, Zbigniew.Zarzycki, Sylwester.Kudzma}@zut.edu.pl

(Received 29 May 2010; revised manuscript received 30 August 2010)

Abstract: This paper is devoted to the problem of energy dissipation and it concerns unsteady friction modeling of the liquid flow in hydraulic lines. One dimensional (1D) quasi-steady model of energy dissipation is in common use. It means that the loss of energy is estimated by the Darcy-Weisbach formulae. Such an approximation is close to reality only for slow changes of the velocity field in the pipe cross-section. In case of fast changes, like fast transients, *e.g.* water hammer, it fails. In this work the wall shear stress τ (defined as an effect of unsteady fluid friction) is presented as a sum of quasi-steady and unsteady components. The unsteady component of the wall shear stress is modeled as a convolution of the local fluid acceleration and a weighting function $w(t)$. The weighting function, in general, makes an allowance for a relation of the historic velocity changes and the unsteady component of the wall shear stress. Primitive weighting functions have usually very complicated structures, and what is more, they make it impossible to perform an efficient simulation of dynamical runs. In this paper, a new weighting function is presented as a sum of exponential components in order to enable efficient calculation of the unsteady component wall shear stress. A few examples of the new effective method of unsteady wall shear stress simulations, in case of the water hammer, are presented. The results of the calculations are compared with experiments known in literature and satisfying results are obtained.

Keywords: unsteady pipe flow, unsteady friction, weighting function

1. Introduction

The contemporary coverage of the unsteady flow in the research of pressurized hydraulic conduits is very extensive and includes without being limited to such issues as the mechanical energy dissipation of fluid, fluid structure interaction or column separation due to cavitation.

This paper is devoted to the first problem and it concerns the modeling of unsteady friction losses for predicting the pressure pulsation in pipes through numerical simulations. The commonly used quasi-steady, one-dimensional model of friction losses based on the Darcy-Weisbach formula can be used in the case of slow changes in a fluid velocity field in a pipe cross-section. However, it fails in the case of a fast-changing flow simulation *e.g.* in the case of the water hammer simulation the received results significantly differ from the results of experimental studies.

The models of unsteady friction losses can be divided into two groups. The first group consists of models based on the instantaneous values of velocity and acceleration. The forerunner in this group was Daily *et al.* [1]. He presented a model in which the term associated with the unsteady shear stress at pipe wall is proportional to the acceleration of liquid. This model was later developed by: Cartens and Roller [2], Safwat and Polder [3], Shuy and Apelt [4]. The model of Brunone *et al.* [5] in which the wall shear stress is proportional not only to the local derivative of the flow velocity but also to its convective derivative falls into this group as well. This model then underwent further modifications (Vitkovsky *et al.* [6], Bughazem and Anderson [7], Bergant *et al.* [8]), mainly by adjusting the coefficients of the local and convective derivatives. On the basis of the dynamic boundary layer thickness Hino *et al.* [9] presented a semi-empirical dependence on the instantaneous coefficient of friction losses for the oscillatory turbulent flow case.

The second group consists of models based on the flow history. The term for the unsteady wall shear stress (and hence the instantaneous coefficient of friction losses) depends on the frequency of changes in the flow and on the pressure. These models reflect relatively well not only the degree of attenuation of the pressure waves but also their shape (in terms of the time course). The forerunner in this group of models was Zielke [10], who presented the instantaneous coefficient of friction losses in the form of an integral convolution of the mean local acceleration of liquid and the weighting function $w(t)$:

$$\lambda_n = \frac{32\nu}{D v^2} \int_0^t \frac{\partial v}{\partial t}(u) w(t-u) du \quad (1)$$

where

- ν – kinematic viscosity;
- D – inner diameter of pipe;
- v – instantaneous mean flow velocity;
- t – time;
- u – time, used in the convolution integral;
- $w(t)$ – weighting function.

This dependence is correct for any changes in the average flow velocity in the pipe cross-section. This model has high time-consuming numerical calculations

due to continuous referring to the flow velocity history. Therefore, it has been simplified by the introduction of the so-called effective weighting functions. It was Trikha [11] who first presented an effective expression of Zielke's weighting model, but this relationship has a limited range of applications. Then, new computing models, based on the approximation of Zielke's weighting function were created by Kagawa *et al.* [12], Suzuki *et al.* [13] and Schohl [14].

However, the presented effective weighting functions still do not cover the whole domain of the dimensionless time of practical engineering applications (especially in the case of a very fast transient flow of a low viscosity liquid in large diameter pipes). Accordingly, a new effective weighting function for the laminar flow is presented in this work. The function has significantly extended the scope of practical applications (the range of dimensionless time is: $10^{-9} \leq \hat{t} \leq \infty$). The most strict model (Zielke [10]) has been used as a base for the process of approximation.

Using the method of characteristics (MOC) for a solution of the equations of motion and continuity there are a few examples of the application of the new weighting function for the waterhammer phenomenon. The results of numerical calculations are compared with the results of experimental studies using the classical experiment data by Holmboe and Rouleau [15] and the experimental data presented by Adamkowski and Lewandowski [16] achieving good agreement.

2. Fundamental equations

The unsteady flow in liquid pipes is often represented by two 1D hyperbolic partial differential equations. The momentum and continuity linearized equations are [17–19]:

$$\rho \frac{\partial v}{\partial t} + \frac{\partial p}{\partial x} + \frac{2}{R} \tau = 0 \quad (2)$$

$$\frac{\partial p}{\partial t} + \rho c^2 \frac{\partial v}{\partial x} = 0 \quad (3)$$

where

- t – time;
- x – the distance along the pipe axis;
- $v = v(x, t)$ – the average value of velocity in the cross-section of a pipe;
- $p = p(x, t)$ – the average value of pressure in the cross-section of a pipe;
- τ – the shear stress at the pipe wall;
- ρ – the density of liquid (constant);
- R – the inside radius of a pipe;
- c – the pressure wave speed.

In the unsteady flow in a pipe, the instantaneous wall shear stress τ may be regarded as the sum of two components [10, 18, 19]:

$$\tau = \underbrace{\frac{\rho \cdot v \cdot |v|}{8}}_{\tau_q} \lambda + \underbrace{\frac{2\mu}{R} \int_0^t w(t-u) \frac{\partial v}{\partial t}(u) du}_{\tau_u} \quad (4)$$

where

- λ – the Darcy-Weisbach friction factor;
- $w(t)$ – the weighting function;
- μ – the dynamic viscosity;
- u – the time, used in a convolution integral.

The first component in Equation (4) τ_q presents the quasi-steady state of the wall shear stress, the second τ_u is the additional contribution due to unsteadiness. Equation (4) relates the wall shear stress to the instantaneous average velocity and to the weighted past velocity changes.

Among the methods which enable to resolve the system of the above equations, particular attention should be paid to the method of characteristics (MOC), which perfectly interprets the essence of the natural phenomena of a transient flow, and at the same time is characterized by fast convergence, easiness to take into account various boundary conditions and the high accuracy of calculation results. With its help one can easily solve a system of partial differential equations of a quasi-linear hyperbolic type (2)–(3) [8, 12, 14, 20, 21].

3. Weighting function models

Zielke presented the weighting functions for a laminar flow [10]:

$$w(\hat{t}) = \sum_{i=1}^6 m_i \hat{t}^{(i-2)/2}, \quad \text{for } \hat{t} \leq 0.02 \tag{5a}$$

$$w(\hat{t}) = \sum_{i=1}^5 e^{-n_i \hat{t}}, \quad \text{for } \hat{t} > 0.02 \tag{5b}$$

where $\hat{t} = \nu \cdot t / R^2$ – the dimensionless time, and:

- | | | |
|-------------------|-------------------|--------------------|
| $m_1 = 0.282095;$ | $m_2 = -1.25;$ | $m_3 = 1.057855;$ |
| $m_4 = 0.9375;$ | $m_5 = 0.396696;$ | $m_6 = -0.351563;$ |
| $n_1 = 26.3744;$ | $n_2 = 70.8493;$ | $n_3 = 135.0198;$ |
| $n_4 = 218.9216;$ | $n_5 = 322.5544.$ | |

Numerical calculations of the time-dependent component of the wall shear stress τ_u (the second component in Equation(4)) can be conducted using the first-order differential approximation [10, 20]:

$$\begin{aligned} \tau_u &= \frac{2\mu}{R} \sum_{j=1}^{k-1} (v_{i,j+1} - v_{i,j}) \cdot w \left((k-j)\Delta t - \frac{\Delta t}{2} \right) = \\ &= \frac{2\mu}{R} \sum_{j=1}^{k-1} (v_{i,k-j+1} - v_{i,k-j}) \cdot w \left(j\Delta t - \frac{\Delta t}{2} \right) \end{aligned} \tag{6}$$

where

- j – the number of the computational time step changing from 1 to k for $k \geq 2$;
- Δt – the time step in MOC.

It is very time consuming to determine the wall shear stress using the above formula (6). Trikha was the first to develop an effective method of solving the integral convolution [11]:

$$\tau_u \approx \frac{2\mu}{R} \sum_{i=1}^n y_i(t + \Delta t) \tag{7}$$

$$y_i(t + \Delta t) = y_i(t) \cdot e^{-n_i \frac{\nu}{R^2} \Delta t} + m_i [v(t + \Delta t) - v(t)] \tag{8}$$

where n_i and m_i are constants of the effective weighting function.

Next, Kagawa *et al.* [12], Suzuki *et al.* [13] and Schohl [14] have improved this method:

- the equation of Kagawa *et al.*:

$$y_i(t + \Delta t) = y_i(t) \cdot e^{-n_i \frac{\nu}{R^2} \Delta t} + m_i \cdot e^{-n_i \frac{\nu}{R^2} \cdot \frac{\Delta t}{2}} \cdot [v(t + \Delta t) - v(t)] \tag{9}$$

- Schohl's equation:

$$y_i(t + \Delta t) = y_i(t) \cdot e^{-n_i \frac{\nu}{R^2} \Delta t} + \frac{m_i \left(1 - e^{-n_i \frac{\nu}{R^2} \Delta t}\right) R^2}{n_i \nu \Delta t} \cdot [v(t + \Delta t) - v(t)] \tag{10}$$

The new effective method (7) however, requires that the weighting function has to be written as a finite sum of exponential expressions:

$$w(\hat{t}) = \sum_{i=1}^k m_i e^{-n_i \hat{t}} \tag{11}$$

The number of exponential terms that make up the final form of the effective weighting function affects the range of its applicability as well as its degree of fit to the classical function (according to Zielke). Over the past 35 years many authors have presented their effective weighting functions for the laminar flow case. Table A1 (in Appendix) presents the ranges of applicability of the effective weighting functions for a laminar flow, while their coefficients estimated are in Table A2 (in Appendix).

The courses of laminar weighting functions are shown in Figure 1.

4. Improved weighting function

In a view of the need to extend the applicability of the effective weighting function, which has been noted by, *inter alia*, Vardy and Brown [22], a new model which is the sum of exponential expressions is presented in the next section of this paper.

The new model is consistent with the classical function by Zielke in the following range of applicability: $10^{-9} \leq \hat{t} < \infty$. The final form of the new function consists of 26 exponential expressions. Since the value of Zielke's weighting function model for the dimensionless time $\hat{t} > 0.02$ is determined from the following formula:

$$w(\hat{t}) = \sum_{i=1}^5 e^{-n_i \hat{t}} \tag{12}$$

where $n_1 = 26.3744$; $n_2 = 70.8493$; $n_3 = 135.0198$; $n_4 = 218.9216$; $n_5 = 322.5544$;

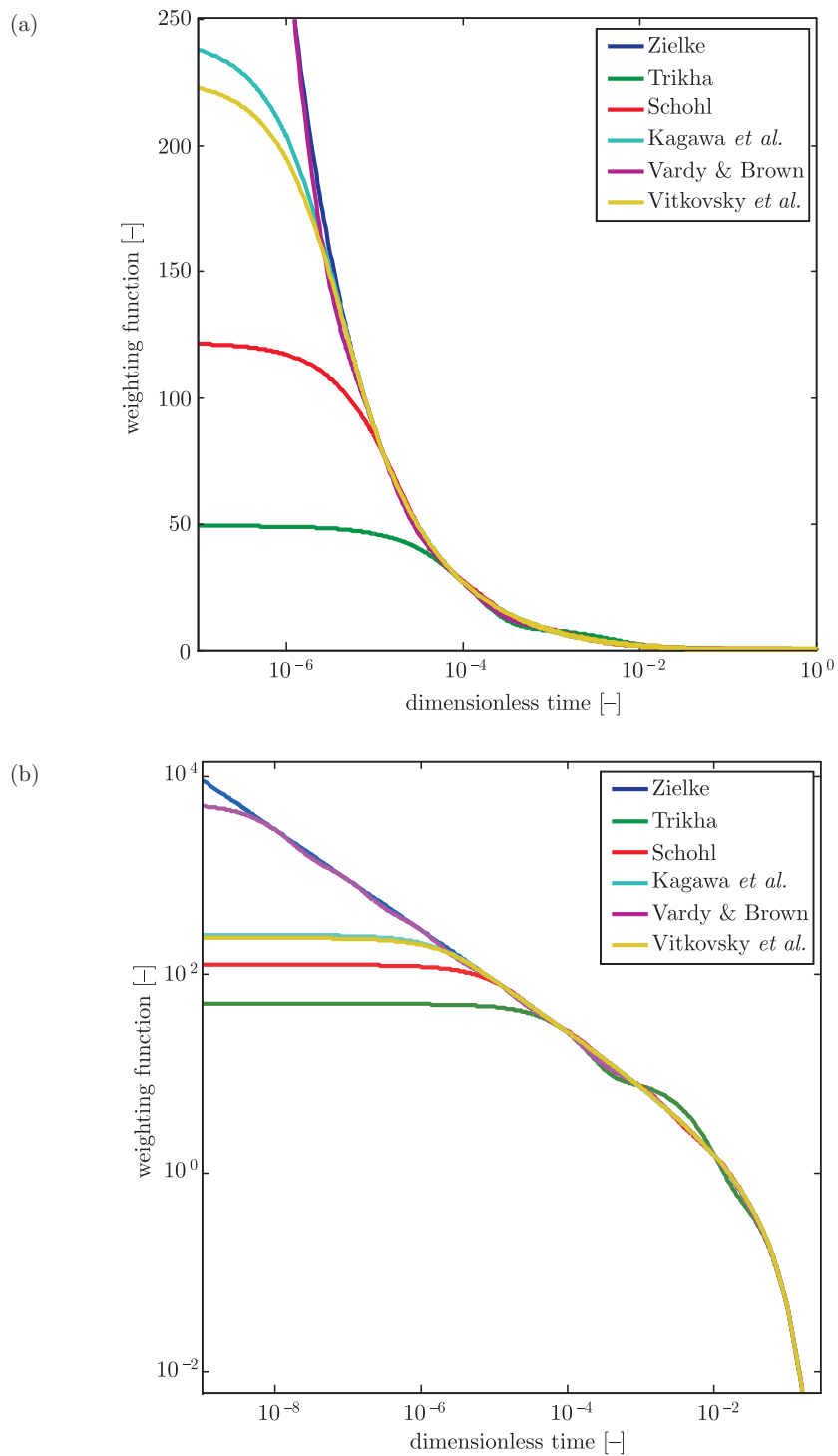


Figure 1. Comparison of laminar function runs: (a) log-linear scale, (b) log-log scale

the first five exponential expressions were to be kept unchanged in this work (so that a perfect fit of a new weighting function in this interval of dimensionless time was received). It was decided to add extra similar components for the mapping of interval $10^{-9} \leq \hat{t} < 0.02$. It was assumed that a very good accuracy would be received by describing each dimensionless time interval $10^{n-1} \leq \hat{t} < 10^n$ with three exponential expressions (the exception was the range $10^{-3} \leq \hat{t} < 0.02$, also describing the three formulas – hence, the worst match of the new weighting function was expected there). In each of those intervals the matching was carried out to uniformly distribute 1000 points, which were the results obtained from using the classic weighting function of Zielke (5).

The effective weighting function coefficients were determined by using the LSQNONLIN function which is a module of MATLAB. The Levenberg-Marquardt algorithm, considered as a one of the most effective minimization algorithms is implemented in this function. It combines the linear approximation away from the minimum and square approximation near the minimum, so that it is specialized to the problems of the method of least squares.

Following the above outlined procedure, all the coefficients of the new effective weighting function for a laminar flow were determined:

$$w_{\text{apr}}(\hat{t}) = \sum_{i=1}^{26} m_i e^{-n_i \hat{t}} \quad (13)$$

where

$m_1 = 1;$	$m_2 = 1;$	$m_3 = 1;$
$m_4 = 1;$	$m_5 = 1;$	$m_6 = 2.141;$
$m_7 = 4.544;$	$m_8 = 7.566;$	$m_9 = 11.299;$
$m_{10} = 16.531;$	$m_{11} = 24.794;$	$m_{12} = 36.229;$
$m_{13} = 52.576;$	$m_{14} = 78.150;$	$m_{15} = 113.873;$
$m_{16} = 165.353;$	$m_{17} = 247.915;$	$m_{18} = 369.561;$
$m_{19} = 546.456;$	$m_{20} = 818.871;$	$m_{21} = 1209.771;$
$m_{22} = 1770.756;$	$m_{23} = 2651.257;$	$m_{24} = 3968.686;$
$m_{25} = 5789.566;$	$m_{26} = 8949.468;$	
$n_1 = 26.3744;$	$n_2 = 70.8493;$	$n_3 = 135.0198;$
$n_4 = 218.9216;$	$n_5 = 322.5544;$	$n_6 = 499.148;$
$n_7 = 1072.543;$	$n_8 = 2663.013;$	$n_9 = 6566.001;$
$n_{10} = 15410.459;$	$n_{11} = 35414.779;$	$n_{12} = 80188.189;$
$n_{13} = 177078.960;$	$n_{14} = 388697.936;$	$n_{15} = 850530.325;$
$n_{16} = 1835847.582;$	$n_{17} = 3977177.832;$	$n_{18} = 8721494.927;$
$n_{19} = 19120835.527;$	$n_{20} = 42098544.558;$	$n_{21} = 92940512.285;$
$n_{22} = 203458923.000;$	$n_{23} = 445270063.893;$	$n_{24} = 985067938.878;$
$n_{25} = 2166385706.058;$	$n_{26} = 4766167206.672.$	

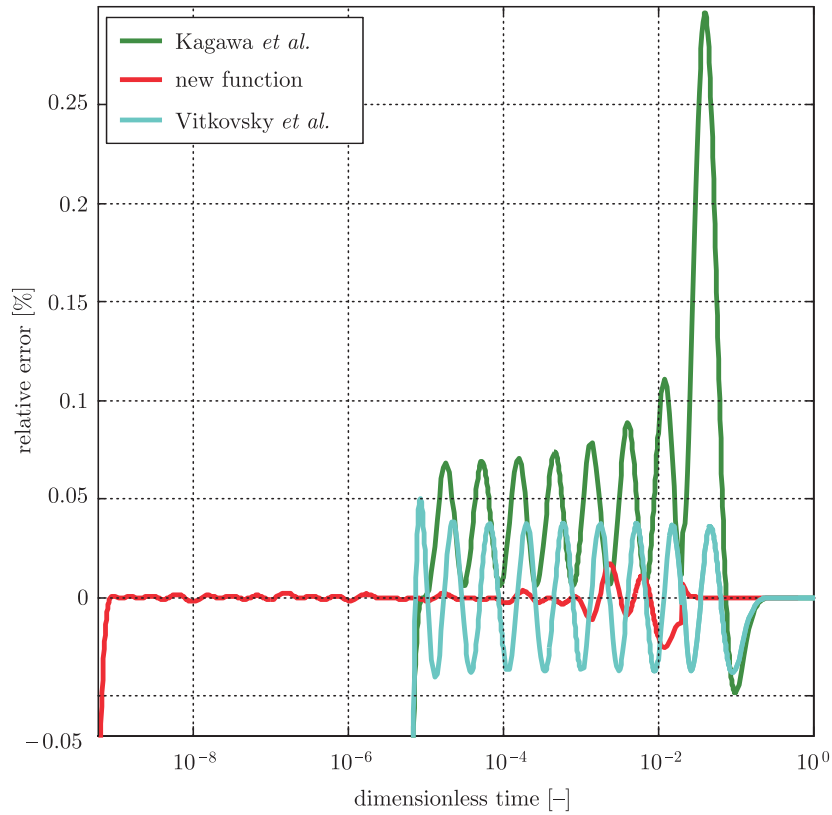


Figure 2. Comparison of weighting functions for laminar flow – relative error percentage

In Figure 2, a comparison of the new weighting function (13) with its inefficient counterpart (Zielke model) is presented in the form of a relative percentage error determined from the following relationship:

$$R_{\text{error}} = \frac{w_{\text{apr}} - w}{w} \cdot 100\% \quad (14)$$

In this figure the best known effective functions from the literature are also presented (Kagawa *et al.* [12], Vitkovsky *et al.* [21]) in order to demonstrate the degree of matching.

A similar weighting function for a turbulent flow with an extended range of applicability will be presented in the next paper.

5. Computation example

In order to compare the accuracy of unsteady (with the use of Zielke's and new weighting function) and quasi-steady models of friction in relation to the experimental data, simulations of a simple waterhammer case (tank – long liquid line and cut-off valve) were conducted.

The computed results were compared with the experimental data reported by Holmboe and Rouleau [15] and Adamkowski and Lewandowski [16].

5.1. Holmboe and Rouleau experiment [15]

Holmboe with Rouleau ran their tests on a copper tube with a radius of 0.0127m and a length of 36.09m connected upstream to a tank which was maintained at a constant pressure by compressed air. The liquid used in the experiment was oil with a viscosity of $39.67 \cdot 10^{-6} \text{ m}^2/\text{s}$. The measured pressure wave speed was 1324.36m/s and the initial flow velocity was 0.128m/s ($\text{Re} = 82$). The downstream valve was rapidly closed in the pipe line during the flow. The pressure fluctuation was measured at the line endpoint (near the valve). It follows from the above parameters that it is a case of a laminar flow. The two models of unsteady hydraulic losses in numerical calculations were used: the Zielke model Equations (5)–(6) and a new effective model, Equations (9) and (13). In addition, a calculation with the use of a quasi-steady model was conducted. The results of the simulations and experimental data are shown in Figure 3.

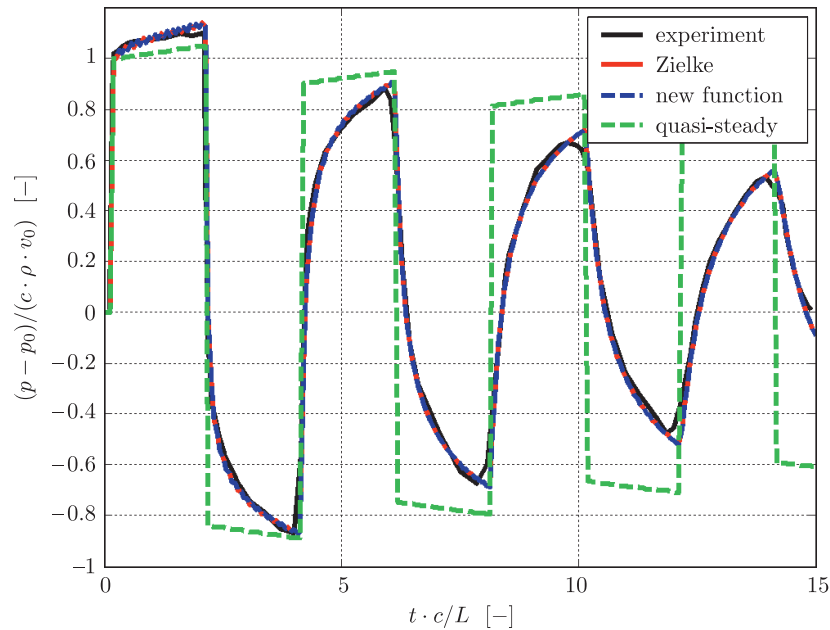


Figure 3. Fluctuations of pressure at line endpoint ($\text{Re} = 82$), Holmboe and Rouleau experiment

It is clearly seen that the calculation using unsteady friction models is much closer to the experimental data. Therefore, in further calculations the unsteady friction models are used instead of the quasi-steady formulae.

5.2. Adamkowski and Lewandowski experiment [16]

Adamkowski's and Lewandowski's experiments were conducted at a test rig specially designed in order to investigate unsteady pipe flows. Its main component was the 98.11m long copper pipe with the internal diameter of 0.016m and wall thickness of 0.001m. The pipe was rigidly mounted to the ground using bearings

in order to minimize its vibrations. A quick-closing, spring driven ball valve was installed at one end of the pipe. The initial conditions were defined by the upstream reservoir pressure head and initial flow velocity in the pipeline. During the tests the water temperature was 22.6°C and the kinematic viscosity coefficient for these conditions was $9.493 \cdot 10^{-7} \text{m}^2/\text{s}$. One run was selected for the purpose of verifying the new unsteady friction model. The initial flow velocity was 0.066m/s ($\text{Re} = 1100$). The results of the simulations and experimental data are shown in Figure 4.

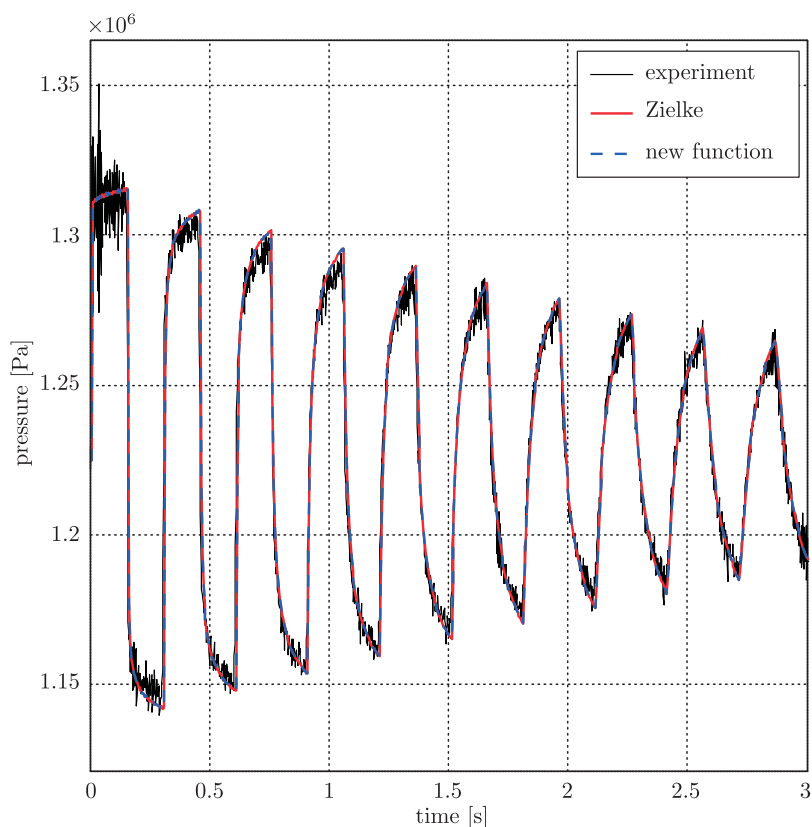


Figure 4. Fluctuations of pressure at line endpoint ($\text{Re} = 1100$), Adamkowski and Lewandowski experiment

It is clear from the above graph that the use of the new efficient weighting function presented in this study (13) ensures the compatibility of results with those obtained from the use of the classical model presented by Zielke.

6. Summary

The main drawback of the classical model presented by Zielke describing the unsteady hydraulic resistance is its inefficiency. In each successive time step more resources are required to the computer's memory (this is due to augmentations in

the quantities of components that make up the sum of the solution of the integral convolutions (6), as well as to the expansion of the matrix which stores information about past velocity changes $v(t)$). Often, after the time when the entire memory of the computer is used, it comes to a forced interruption of the performance simulation. Hence, the classic weighting functions that make the obtained results coincide with the results of the experimental studies, and even today, with the tremendous development of the computer technology, fit only to simulate very short transients.

The known efficient solution of the integral convolution [12, 14] allowed, in case of using a weighting function as a finite sum of the exponential terms ($m_i e^{-n_i \hat{t}}$), a significant reduction in the computation time and reducing the demand for the operational memory. What is important in increasing the number of time steps calculation, computation time increases linearly, as is shown in Figure 5 (calculations were carried out on a laptop computer – Compaq Presario 2100 mobile AMD Athlon™ XP2200+, 192 MB RAM). It was also the impact of the number of the weighting function terms on the time of calculation that was investigated. The two cases are presented in Figure 5: 10 terms and 26 terms

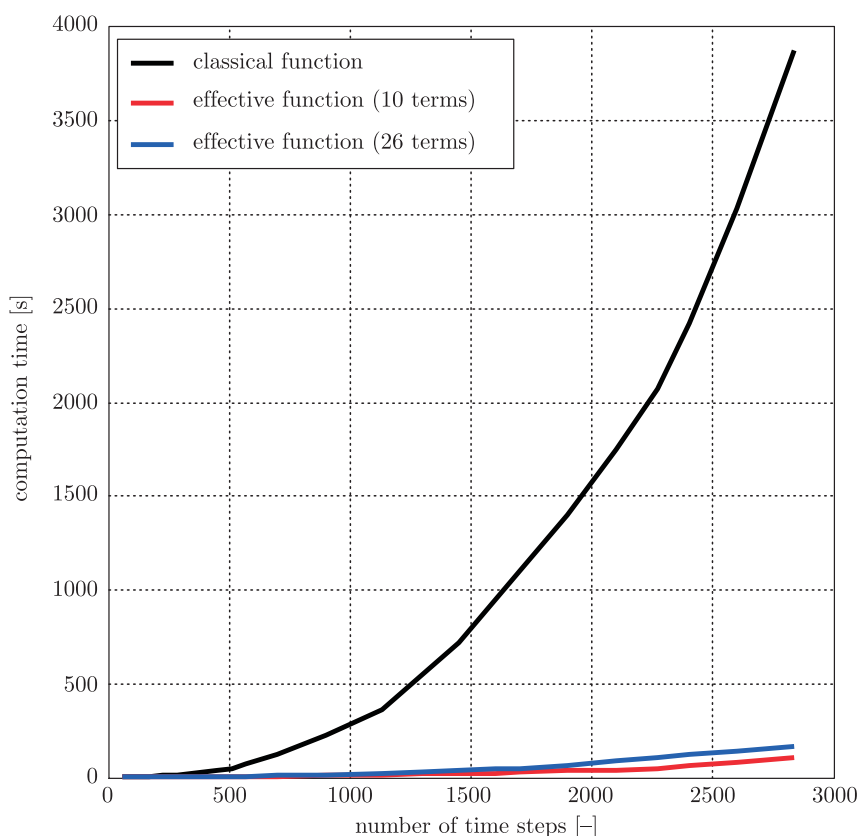


Figure 5. Time of numerical calculations, depending on the number of time steps used

function. The increase in the time consumption for these cases is very small in relation to the classical model.

Numerous numerical tests, carried out by the authors have revealed that the simulation results using models with small ranges of applicability (*e.g.* by Trikha) often deviate from the experimental results (as a result of going beyond the scope of applicability of the used weighting function). Professional software, which may in future be based on the weighting function presented in this work must prevent crossing outside the range of its applicability – by informing the user about the need to change the numerical parameters (*e.g.* the number of the simultaneously observed pipe cross sections).

The presented new weighting function characterized by an extended range of applicability in the domain of dimensionless time are suitable for the efficient modeling of transient laminar flows. The studies show that the results of the numerical simulations, in which a new weighting function was used, overlap with those that use the classic Zielke model.

In the next stage of research the usefulness of the new weighting function presented in this paper to simulate transients with cavitation should be also explored.

References

- [1] Dailey J W, Hankey W L, Olive R W and Jordaan J M 1956 *J. Basic Eng.* **78** 1071
- [2] Carstens M R and Roller J E 1959 *ASCE J. Hydraulics Div.* **85** (HY2) 67
- [3] Safwat H H and Polder Jaap van Den 1973 *J. Fluids Eng.* **95** 91
- [4] Shuy E B and Aplet C J 1987 *Conf. on Hydraulics in Civil Eng.*, Melbourne, Australia, pp. 137–141
- [5] Brunone B, Golia U M and Greco M 1991 *Proc. Int. Meeting on Hydraulic Transients with Column Separation, 9th Round Table*, IAHR, Valencia, Spain, pp. 201–209
- [6] Vitkovsky J, Lambert M, Simpson A and Bergant A 2000 *Proc. 8th Int. Conf. Pressure Surges, BHR Group Conf. Series Publ.*, Hague, Netherlands, pp. 471–482
- [7] Bughazem M B and Anderson A 2000 *Proc. 8th Int. Conf. Pressure Surges, BHR Group Conf. Series Publ.*, Hague, Netherlands, pp. 483–498
- [8] Bergant A, Simpson A and Vitkovsky J 2001 *J. Hydraulic Res.*, IAHR, **39** (3) 249
- [9] Hino M, Sawamoto M and Takasu S 1977 *Trans. of JSCE* **9** 282
- [10] Zielke W 1968 *J. ASME* **90** 109
- [11] Trikha A K 1975 *J. Fluids Eng.*, Trans. ASME, **97** 97
- [12] Kagawa T, Lee I, Kitagawa A and Takenaka T 1983 *Trans. Jpn. Soc. Mech. Eng., ser. A* **49** (447) 2638 (in Japanese)
- [13] Suzuki K, Taketomi T and Sato S 1991 *J. Fluids Eng.*, Trans. ASME, **113** 569
- [14] Schohl G A 1993 *J. Fluids Eng.*, Trans. ASME, **115** 420
- [15] Holmboe E L and Rouleau W T 1967 *J. Basic Eng.*, Trans. ASME, ser. D, **89** (11) 174
- [16] Adamkowski A and Lewandowski M 2006 *J. Fluids Eng.*, Trans. ASME, **128** (6) 1351
- [17] Ohmi M, Kyomen S and Usui T 1985 *Bull. JSME* **28** (239) 799
- [18] Zarzycki Z 1994 *A Hydraulic Resistance's of Unsteady Liquid Flow in Pipes*, Technical University of Szczecin, Szczecin, Poland, **516** (in Polish)
- [19] Zarzycki Z 2000 *Proc. 8th Int. Conf. on Pressure Surges*, BHR Group Conf. Series, Hague, Netherlands, **39**, pp. 529–534
- [20] Zarzycki Z and Kudźma S 2004 *Proc. 9th Int. Conf. on Pressure Surges*, BHR Group, Chester, UK, pp. 439–455



-
- [21] Vitkovsky J P, Stephens M L, Bergant A, Simpson A R and Lambert M F 2004 *9th Int. Conf. on Pressure Surges*, Chester, UK, pp. 405–419
- [22] Vardy A E and Brown J M B 2004 *J. Hydraulic Eng.*, ASCE, **130** (11) 1097



Appendix

Table A1. Ranges of applications of effective weighting functions

Model	Trikha's model [11]	Schohl's model [14]	Model of Kagawa et al. [12]	Model of Vitkovsky et al. [21]	Model of Vardy & Brown [22]
Range of application	$7.41 \cdot 10^{-5} \leq \hat{t} \leq 10^1$	$1.26 \cdot 10^{-5} \leq \hat{t} \leq 10^0$	$6.31 \cdot 10^{-6} \leq \hat{t} \leq \infty$	$6.31 \cdot 10^{-6} \leq \hat{t} \leq \infty$	$10^{-8} \leq \hat{t} \leq \infty$

Table A2. Estimated coefficients of effective laminar weighting functions

i	Trikha's model [11]		Schohl's model [14]		Model of Kagawa et al. [12]		Model of Vitkovsky et al. [21]		Model of Vardy & Brown [22]	
	m_i	n_i	m_i	n_i	m_i	n_i	m_i	n_i	m_i	n_i
1	1	26.4	1.051	26.65	1	26.3744	1	26.3744	1	26.3744
2	8.1	200	2.358	100	1.16725	72.8033	1.09301	72.044	2.1830	10^2
3	40	8000	9.021	669.6	2.20064	187.424	1.82206	166.931	2.714	$10^{2.5}$
4			29.47	6497	3.92861	536.626	3.34085	435.932	7.5455	10^3
5			79.55	57990	6.78788	1570.60	5.89377	1229.74	39.0066	10^4
6					11.6761	4618.13	10.2835	3584.84	106.8075	10^5
7					20.0612	13601.1	17.9006	10621.7	359.0847	10^6
8					34.4541	40082.5	31.1516	31757	1107.9295	10^7
9					59.1642	118153	54.4168	95563.7	3540.683	10^8
10					101.59	348316	99.4360	293268		